Radiocarbon (2024), **66**, pp. 498–517
doi:10.1017/RDC.2024.64

CAMBRIDGE UNIVERSITY PRESS

RESEARCH ARTICLE

Sequencing the Southern Iberian Late Neolithic hypogeum cemetery of La Beleña through radiocarbon dating and Bayesian modeling

Jonathan Santana[1], José L Caro[2], María D Camalich Massieu[3], Gonzalo Aranda Jiménez[4] and Dimas Martín Socas[3]

[1]Department of Historical Sciences, University of Las Palmas de Gran Canaria, Spain, [2]Department of Languages and Computer Science, University of Málaga, Spain, [3]Department of Geography and History, Prehistory Area, University of La Laguna, Spain and [4]Department of Prehistory and Archaeology, University of Granada, Spain
Corresponding author: Jonathan Santana; Email: jonathan.santana@ulpgc.es

Received: 16 May 2023; **Revised:** 11 January 2024; **Accepted:** 15 March 2024

Keywords: Bayesian modeling; collective burials; hypogeum; Iberian Peninsula; Late Neolithic

Abstract
This study aims to determine the chronological sequence of the collective burials in the hypogea of the prehistoric cemetery of La Beleña (Cabra, Córdoba) through Bayesian analyses of ^{14}C dates obtained from human remains. The data from this site are not only key to grasping the phenomenon of the introduction and spread of hypogea throughout the western Mediterranean, but to gain insight into multi-stage funerary practices during the Late Neolithic/Chalcolithic. The dataset comprises ^{14}C dates of 71 of the 79 individuals placed in five of La Beleña's six hypogea. The findings suggest: (i) La Beleña is one of the oldest assemblages of hypogea in Iberia, (ii) that this type of collective burial spread rapidly throughout the western Mediterranean area, (iii) that La Beleña is marked by two main phases of funerary activity interspersed by brief burial surges, (iv) funerary intensity at La Beleña increased between cal BC 3400–2900 (2σ), and (v) the cemetery saw a very brief surge of burials potentially related to a catastrophic event. The results of this analysis thus shed light on the little-known chronological sequence of prehistoric hypogea or rock-cut tombs in Iberia, their spread, and their relation to other Late Neolithic collective burials in western Europe.

Introduction

Collective burials are characteristic of western Europe's Late Neolithic (Chambon et al 2018). This practice appears to have its origins in the late 5th millennium BC in Brittany from where it expanded in the early 4th millennium BC to Britain and Ireland, northern Europe and Iberia (Balsera et al 2015; Scarre et al 2003; Schulz Paulsson 2019; Whittle et al 2011). Collective burials are defined as single features containing multiple corpses that contrary to mass burials were deposited over periods of time ranging from several decades to hundreds of years. The dead were often accompanied by a variety of goods such as pottery, stone tools and ornaments, items potentially reflecting differences of social status (Chambon et al 2018). The reasons behind the phenomenon remain unclear. Certain scholars argue they reflect the emergence of complex societies and their need to reinforce and display social identity and alliances through funerary practices (Boulestin 2016; Sánchez-Quinto et al 2019). Others suggest they relate to a change in religious beliefs, with an emphasis on community and collective afterlife (Whittle 2017).

The tradition of collective burials intensified from around cal BC 3500 to 2500 throughout western Europe as well among different central Mediterranean islands (Aranda Jiménez et al 2022; Chambon

et al 2018; Thompson et al 2020). They are associated with megalithic features such as barrows, cairns, as well as natural and artificial caves (rock-cut tombs/hypogea) (Chambon et al 2018; Pardo-Gordó and Carvalho 2020; Scarre 2010). However, grasping the nexus between their different architectural features is complex due to multiple factors such as chronology, local traditions and geomorphological conditions (Guilaine 2021; Sauzade 2021). Furthermore, the tradition of collective burials persisted, albeit with changes, into the Early Bronze Age. A notably difference is a decrease in the number of individuals in the tombs and that the dead tended to receive a more individualised treatment suggesting a shift in this direction by society (Aranda Jiménez et al 2017; Chambon et al 2018).

Hypogea are among the least known types of prehistoric collective burials. Their origin and spread throughout western Europe are still the subject of debate due to the scarcity of high-precision ^{14}C dates (Guilaine 2015; Sauzade 2021). Rock-cut tombs in the central Mediterranean such as at Cuccuru S'Arriu in Sardinia (Robin et al 2021) and Scintilia in Sicily (Gullì and Terrasi 2020) date to approximately cal BC 4500. These types of features subsequently became widespread throughout these two islands around cal BC 4000–3400 (Robin et al 2021). Similar features are recorded in the Iberian Peninsula and in Provence in the first half of the 4th millennium BC (Carvalho 2014; Guilaine 2015; Sauzade 2021). However, how this practice spread throughout continental western Europe remains obscure. The current radiometric data (cal BC 3700–3550) suggest the Portuguese cemeteries of Quinta da Abóboda, Barrancas I and Sobreira de Cima as the earliest hypogea in the Iberian Peninsula (Valera 2013, 2020a). Furthermore, these collective burials became more common around cal BC 3400–2900 during southern Iberia's transition from the Late Neolithic to the Chalcolithic (Guilaine 2015; Lillios et al 2014). The end of the tradition of rock-cut tomb cemeteries is likewise unclear as certain hypogea, subsequent to a hiatus, saw reuse by Bell Beaker groups (Valera et al 2014).

As other prehistoric collective burials, hypogeum cemeteries are highly dynamic spaces characterised over time by multiple depositional and postdepositional events yielding complex palimpsests of funerary practices (Chambon et al 2018). The disturbance of their primary and secondary burials in the form of trampling, intentional fragmentation, bone removal, translocation and secondary disposal have yielded intricate, multi-chronological archaeological contexts complicating their sequencing (Aranda Jiménez et al 2020a; Lillios et al 2014; Valera 2013). In spite of these complications, fine-grained chronometric analyses of prehistoric collective burials have enabled gaining an unprecedented understanding of their dynamics (Scarre 2010). These approaches consist of interdisciplinary analyses based on three main strategies: 1) radiocarbon (^{14}C) datings of human remains so as to associate the isotopic events reflected by the radiometric measurements (that is, the moment of death) to the depositional event (when the individual was placed in the tomb); 2) applying sampling criteria based on dating a minimum number of individuals (MNI) whose selection stems from osteological analyses; and 3) designing Bayesian models to estimate the outset, duration and end of the events (Aranda Jiménez et al 2017, 2021; Bayliss 2009; Blank et al 2020).

The exponential growth of direct accelerator mass spectrometry (AMS) datings of human remains has revitalised this research as it offers solid foundations to delve into the lifespan and abandonment of these features. The new data also shed light on the links of the manipulations of human remains and other funerary practices such as the opening and closing of these spaces (Aranda Jiménez et al 2022). The new approaches likewise allow renewing work on older tombs that at their moment of their excavation did not benefit from these techniques (Aranda Jiménez et al 2017, 2020b; 2021; Schulting et al 2017). Recent work on prehistoric megalithic collective burials in the Iberian Peninsula clearly demonstrates the impact of both ^{14}C dates and Bayesian modelings on their interpretation (Aranda Jiménez et al 2017, 2020a, 2021, 2022; García Sanjuán et al 2018; Linares-Catela and Vera-Rodríguez 2021; Santa Cruz del Barrio et al 2020; Valera 2020a; Valera et al 2019). These methods have led to unravelling the use, closure, and reuse of these monuments as well clarifying their multi-stage burial practices. These new techniques have likewise contributed to gaining a finer grasp of the chronological framework of the Iberian phenomenon as they offer clues to the origin, spread and interaction of the different types of megalithic monuments and hypogea from the architectural standpoint.

https://doi.org/10.1017/RDC.2024.64 Published online by Cambridge University Press

The radiometric analyses and Bayesian modeling of the hypogea of La Beleña specifically offer a chronological framework shedding light on its multi-stage funerary practices as well as the spread of this phenomenon throughout the western Mediterranean landscape. Furthermore, this study counts on one of Europe's largest ^{14}C datasets which help to fill the research gap concerning the spread of prehistoric hypogea or rock-cut tombs throughout Iberia and the ties of these features to other Late Neolithic collective burials of western Europe.

Archaeological background

The cemetery of La Beleña was initially discovered in 1973 during agricultural work which led to the collapse of the dome-shaped ceiling one of its tombs (Hypogeum 1). The exact location of this hypogeum is still uncertain due to modifications made to the area following its discovery. However, locals who visited the site in the 1970s indicated that the hypogeum was situated just a few meters south of Hypogeum 2. The opening in the ground revealed human bones and grave goods that were removed by the local archaeologist and deposited in the Museum of Archaeology of Cabra. A second well-preserved hypogeum was later discovered by an agricultural worker in 2015. This find led to a research project aimed at identifying the site's burial practices, chronological framework and osteobiography of the dead. Since then, five new rock-cut tombs or hypogea were identified and excavated (Figure 1b) (Camalich et al 2023).

The hypogea of Beleña contain primary and secondary human depositions and grave goods. Their burial chambers are hemispherical connected to west-facing corridors cut into a compact marl substrate. Although the ceiling of three collapsed during recent agricultural work (20th century), their contents suffered no damage (Figure 2). Moreover, the archaeological fieldwork identified evidence of intentional sealing in Late Neolithic/Chalcolithic ending their use (Camalich et al 2023).

Material and methods

Material

La Beleña comprises four primary inhumations linked to Hypogea 3 and 5. Otherwise all hypogea contain commingled human remains in secondary position. The primary inhumations, determined by the articulated arrangement of their bones, consist of individuals buried soon after their death. This means their ^{14}C dates closely align with the time when their remains were deposited. The other dispersed commingled bones, in turn, stem from secondary multi-stage burial practices meaning there is no direct chronological link between their ^{14}C dates and the moment/s of their disposal.

The sampling strategy intended to grasp the dynamics of the funerary activity was intended to analyse the largest number of human remains (Santana 2020). The approach, based on the minimum number of individuals, was to ensure that the same individual was not sampled twice. The osteological collection was systematically analysed to establish the paleodemographic profile and to identify other features, including paleopathological disorders and trauma. Teeth analyses yielded an MNI of 79 individuals for the five tombs, a total that slightly surpasses that of the cranial and infracranial analyses, respectively 62 and 67 (Table 1). As several individuals were only represented by teeth, not all were subjected to ^{14}C analyses as certain were reserved for ancient DNA analyses. Ultimately ^{14}C analyses were carried out on a total 71 individuals, broken down into 52 bone fragments and 19 teeth (Tables 1–2).

Methods

Radiocarbon analyses

The ^{14}C dates were obtained by Accelerator Mass Spectrometry (AMS) at the Beta Analytic Testing Laboratory (USA) and at the Centro Nacional de Aceleradores (Spain). The results were then subjected to Bayesian modeling. OxCal software version 4.4 (Bronk Ramsey 2009a) served to design the

https://doi.org/10.1017/RDC.2024.64 Published online by Cambridge University Press

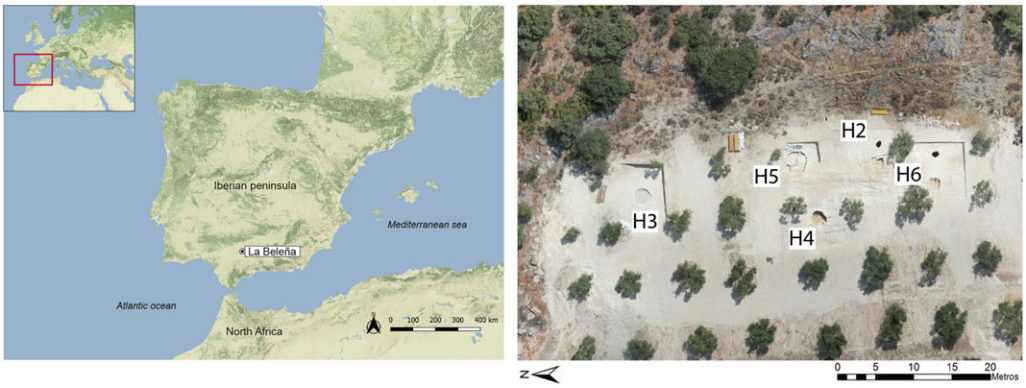

Figure 1. *Map of the Iberian Peninsula with the location of the cemetery of La Beleña (left) and aerial view of the five hypogea (right).*

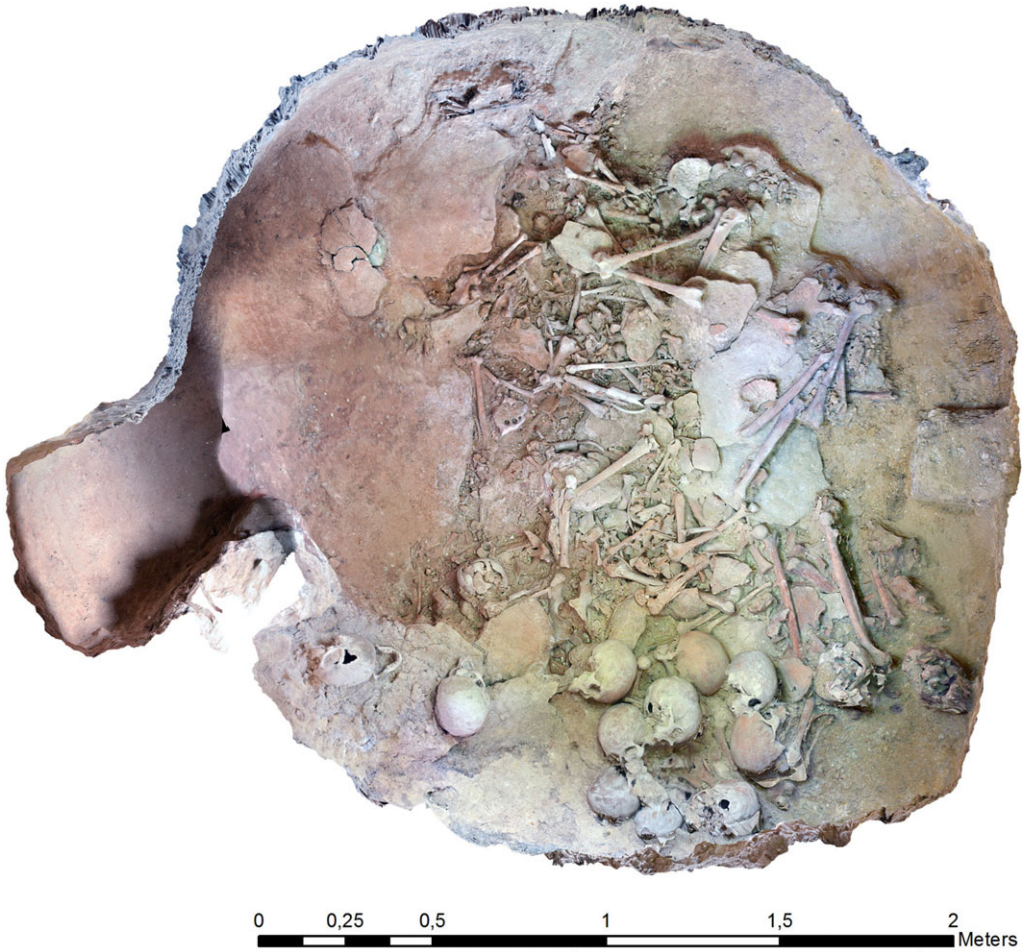

Figure 2. *View of Hypogeum 2 containing displaced commingled human remains in secondary position. The cranial and infracranial elements were arranged in separate groups.*

https://doi.org/10.1017/RDC.2024.64 Published online by Cambridge University Press

Table 1. *La Beleña: minimum number of individuals by hypogeum based on teeth and skeletal region analyses. The final column indicates the number retained for AMS ^{14}C dating*

Hypogeum	MNI teeth	MNI crania	MNI infracranial	AMS dating
2	22	20	21	21
3	13	5	7	7
4	9	6	7	9
5	16	11	16	15
6	19	19	16	19
Total	79	62	67	71

calibrations, plots and modelings. The 2σ levels of confidence, recommended by Millard (2014), served as the base when discussing the ^{14}C measurements. 1σ probability intervals were added to the figures and tables. The modeled dates are rounded to the nearest five years since the modeled results vary from run to run. The ^{14}C dates of individuals linked to terrestrial diets were corrected by the international IntCal20 atmospheric calibration curve (Reimer et al 2020).

Stable isotope analyses

Stable isotope analyses ($\delta^{13}C$ and $\delta^{15}N$) were likewise carried out to evaluate marine/freshwater intake. The consumption of significant amounts of these types of resources can produce what is known as the reservoir effect, skewing the precision of the datings, that is, yielding earlier measurements (Cook et al 2015). Stable isotope analyses were thus carried out by elemental analysis – isotope ratio mass spectrometry (EA-IRMS) from samples of bone and dentine collagen (50 bone and 19 dentine samples). The isotopic value analyses were undertaken by Beta Analytic Inc. (USA), ETH Zurich Laboratory of Ion Beam Physics (CH) and the IsoAnalytical Laboratory (UK) (Table 2). The three laboratories adhered to rigorous quality control guidelines applying international reference standards. Differences between laboratories can influence the comparability of isotope values from one lab to another (Pestle et al 2014). Nevertheless, collagen isotope readings tend to be consistent across various labs, especially when identical preparation techniques are employed. The isotopic values were reported according to the international V-PDB standards for $\delta^{13}C$ and atmospheric air (AIR) for $\delta^{15}N$. The quality of the collagen extracted from the bones was controlled by international criteria yielding > 1% and a C:N ratio of 2.9–3.6 (van Klinken 1999).

Bayesian modeling

Bayesian models yield rigorous estimates of the start, end and duration of events (Bayliss 2015; Bayliss et al 2007a). The current study assumes that the human remains were deposited soon after their death. Long-term curation and/or retrieval of human bones can also be detected through these types of models in the form of outliers (Schulting et al 2017).

Several models were drawn up with the OxCal software based on the different interpretations of the ^{14}C dataset. A *Single Uniform Phase Model* (Bronk Ramsey 2009a) determined whether all the burials were devoid of discontinuity and align with a single chronological phase. This therefore equates with a uniform distribution model based on the hypothesis that all the events are likely to occur at any time at the start and end of the potential phases. Hence calibrated models were created for each hypogeum using OxCal tools (Oxcal's *Sequence, Phase, Boundary, Duration, Interval, and Difference commands*; Bronk Ramsey 2009a, 2009b). The efficacy of each model is signified by the agreement indices, specifically A_{model} and $A_{overall}$, both of which should not fall below a threshold of 60%. A_{model} furnishes a comprehensive metric evaluating the congruence of the entire model, while $A_{overall}$ operates as a composite function of the individual agreement indices for each specific date (Bronk Ramsey 2009a).

https://doi.org/10.1017/RDC.2024.64 Published online by Cambridge University Press

Table 2. *La Beleña: results of the ^{14}C datings and isotope analyses*

														Unmodeled calibrated dates	
Hypogeum	ID	Individual	Sex	Age	Sample	Type	^{14}C Lab code	%C	%N	C:N	$\delta^{13}C$	$\delta^{15}N$	Date BP	sd	Cal BC 1σ (1σ)	Cal BC 2σ (2σ)
H2	161	9	Male	Adult	Tooth	FDI 14	CNA-3768	—	—	3,2	—	—	4547	31	3365–3115	3370–3100
H2	395	13	Female	Adult	Bone	Cranium	CNA–3762	38,7	14,0	3,2	–20,0	8,1	4523	31	3355–3105	3360–3100
H2	54	1	Female	Adult	Tooth	FDI 27	CNA–3765	—	—	3,2	—	—	4519	32	3350–3105	3360–3100
H2	56	3	Female	Adult	Bone	Cranium	ETH-82483	38,1	13,6	3,2	–19,7	8,8	4510	23	3345–3105	3350–3100
H2	58	5	Male	Adult	Bone	Cranium	CNA–3761	38,6	14,1	3,2	–19,4	9,4	4499	31	3340–3105	3355–3095
H2	61	7	Male	Adult	Bone	Cranium	CNA–3759	42,7	15,6	3,2	–19,7	9,4	4491	30	3330–3105	3350–3040
H2	729	21	Male	Adult	Bone	Mandible	Beta-421160	37,5	13,6	3,2	–19,8	8,4	4480	30	3330–3100	3340–3030
H2	320	11	Female	Adult	Bone	Cranium	CNA–3764	42,4	15,5	3,2	–19,6	8,2	4478	30	3330–3095	3340–3030
H2	59	6	Male	Adult	Bone	Cranium	CNA–3760	44,1	16,4	3,1	–20,5	7,5	4465	31	3325–3035	3340–3025
H2	55	2	Female	Adult	Bone	Cranium	ETH-82484	36,2	12,9	3,2	–19,4	9,6	4443	23	3310–3025	3330–2935
H2	57	4	Female	Adult	Bone	Cranium	CNA–3766	38,6	14,1	3,2	–19,2	11,3	4437	32	3315–3015	3330–2930
H2	160	19	Unknown	Non-adult	Bone	Cranium	ETH-82486	20,7	7,4	3,2	–20,0	7,9	4430	23	3265–3015	3320–2930
H2	1037	17	Unknown	Non-adult	Bone	Cranium	ETH-82487	38,1	13,5	3,2	–19,0	9,7	4428	23	3265–3010	3320–2925
H2	962	12	Unknown	Non-adult	Bone	Cranium	ETH-82485	40,3	14,3	3,2	–19,7	7,0	4417	23	3095–2940	3310–2920
H2	272	10	Unknown	Non-adult	Tooth	FDI 46	Beta-421161	37,5	13,4	3,2	–19,8	8,5	4400	30	3085–2930	3265–2910
H2	334	15	Male	Adult	Bone	Cranium	ETH-82482	—	—	3,2	—	—	4398	29	3085–2930	3260–2915
H2	1017	16	Female	Adult	Bone	Cranium	CNA–3763	45,5	16,5	3,2	–19,7	8,3	4396	31	3080–2930	3265–2910
H2	111	8	Unknown	Non-adult	Bone	Cranium	CNA-3767	37,3	13,5	3,2	–20,1	8,0	4379	32	3020–2925	3095–2910
H2	728	20	Unknown	Adult	Tooth	FDI 46	Beta-421162	42,3	15,4	3,2	–19,7	7,8	4300	30	2920–2890	3010–2880
H2	997	14	Female	Adult	Bone	Cranium	ETH-82481	37,5	13,4	3,2	–20,0	7,7	4300	30	2920–2890	3010–2880
H2	358	18	Female	Adulto	Bone	Mandible	Beta-421159	38,5	14,1	3,2	–19,2	11,3	4290	30	2915–2890	3010–2875
H3	2254	1	Unknown	Adult	Bone	Fibula	Beta-465703	42,5	15,4	3,2	–19,2	8,2	4510	30	3345–3105	3355–3100
H3	2114-4	4	Unknown	Adult	Tooth	FDI 26	Beta-593533	41,8	15,0	3,2	–19,3	7,8	4510	30	3345–3105	3355–3100
H3	2226-1	2	Unknown	Adult	Tooth	FDI 43	Beta-465702	44,6	16,3	3,2	–18,7	9,3	4500	30	3330–3090	3340–3025
H3	2157	5	Unknown	Adult	Tooth	FDI 26	Beta-593532	42,3	14,9	3,3	–19,1	9,4	4470	30	3335–3105	3350–3095
H3	2063	7	Unknown	Adult	Tooth	FDI 26	Beta-593530	41,9	15,0	3,3	–19,9	7,9	4450	30	3320–3025	3335–2940
H3	2178-1	6	Unknown	Adult	Tooth	FDI 26	Beta-593531	41,7	15,1	3,2	–19,2	7,2	4420	30	3100–2935	3320–2920
H3	2178-4	3	Unknown	Adult	Tooth	FDI 42	Beta-465701	42,3	15,4	3,2	–19,7	7,7	4420	30	3260–2935	3320–2920
H4	3116	1	Unknown	Adult	Tooth	FDI 46	Beta-465699	42,2	15,2	3,2	–19,0	8,9	4460	30	3325–3030	3335–3020
H4	3112-1	5	Unknown	Adult	Bone	Mandible	Beta-593538	42,1	15,1	3,2	–18,9	7,6	4440	30	3315–3105	3330–2930
H4	3098	7	Unknown	Adult	Bone	Mandible	Beta-593536	41,4	14,6	3,3	–18,8	9,7	4420	30	3100–2935	3320–2920
H4	3133-3	8	Unknown	Adult	Tooth	FDI 26	Beta-593535	41,9	15,0	3,3	–19,6	8,9	4420	30	3100–2935	3320–2920
H4	3148-1	3	Unknown	Adult	Bone	Cranium	Beta-465700	41,4	14,7	3,3	–19,6	8,0	4400	30	3085–2930	3280–2910
H4	3104-2	9	Unknown	Adult	Tooth	FDI 26	Beta-593534	41,8	15,1	3,2	–19,1	9,9	4370	30	3010–2920	3090–2905
H4	3170–2	6	Unknown	Adult	Tooth	FDI 26	Beta-593537	41,6	15,0	3,2	–19,6	8,5	4360	30	3010–2915	3085–2905

(*Continued*)

Table 2. (*Continued*)

Hypogeum	ID	Individual	Sex	Age	Sample	Type	^{14}C Lab code	%C	%N	C:N	δ^{13}C	δ^{15}N	Date BP	sd	Unmodeled calibrated dates	
															Cal BC 1σ (1σ)	Cal BC 2σ (2σ)
H4	3160	4	Unknown	Adult	Bone	Mandible	Mandible	41,4	14,6	3,3	–19,7	8,7	4340	30	3010–2905	3070–2895
H4	3112-1	2	Unknown	Adult	Bone	Cranium	Beta-465704	41,3	14,6	3,3	–19,5	7,7	4310	30	3000–2890	3010–2885
H5	5695-2	16	Unknown	Adult	Bone	Cranium	Beta-593540	44,1	14,2	3,6	–19,9	9,4	5250	30	4215–3990	4230–3980
H5	4243	11	Unknown	Adult	Tooth	FDI 26	Beta-593546	43,1	14,7	3,4	–19,3	8,6	4880	30	3700–3635	3755–3540
H5	5535	9	Unknown	Adult	Tooth	FDI 26	Beta-593548	42.4	15,0	3,3	–19,6	9,2	4840	30	3650–3535	3700–3530
H5	5281	10	Unknown	Adult	Tooth	FDI 26	Beta-593547	42,3	14,8	3.3	–20,1	8,0	4790	30	3635–3530	3640–3525
H5	5058	14	Male	Adult	Tooth	FDI 26	Beta-593542	42,1	15,1	3,3	–17,9	8,9	4580	30	3485–3195	3495–3105
H5	6111	13	Unknown	Adult	Bone	Cranium	Beta-593543	41,9	14,8	3,3	–19,2	9,0	4560	30	3370–3130	3490–3105
H5	5423	7	Unknown	Adult	Tooth	FDI 13	Beta-481434	41,9	15,3	3,2	–19,4	8,7	4500	30	3335–3105	3350–3095
H5	4451	8	Unknown	Adult	Tooth	FDI 13	Beta-481430	41,8	15,1	3,2	–19,3	8,0	4470	30	3330–3045	3340–3025
H5	5110–10	2	Female	Adult	Bone	Cranium	Beta-481432	41,7	15,2	3,2	–19,8	8,3	4470	30	3330–3045	3340–3025
H5	5199-1	15	Unknown	Adult	Tooth	FDI 26	Beta-593541	41,6	15,0	3,2	–18,2	9,6	4410	30	3090–2935	3315–2915
H5	4942	1	Male	Adult	Bone	Cranium	Beta-481428	42,7	15,2	3,3	–19,2	9,0	4390	30	3075–2925	3095–2915
H5	4881	3	Male	Adult	Bone	Fibula	Beta-481431	38,6	13,8	3,3	–19,0	9,1	4380	30	3020–2925	3090–2910
H5	5273	12	Unknown	Adult	Bone	Cranium	Beta-593544	41,6	14,7	3,3	–19,2	9,7	4360	30	3010–2915	3085–2900
H5	6199	5	Unknown	Adult	Bone	Cranium	Beta-571872	40.8	14.7	3.2	–19,7	8,4	4360	30	3010–2915	3085–2900
H5	5126	4	Unknown	Non-adult	Bone	Cranium	Beta-481429	42,0	14,8	3,3	–19,4	8,2	4310	30	3000–2890	3010–2885
H6	8533	11	Unknown	Adult	Bone	Cranium	Beta-533965	41,5	15,1	3,2	–19,6	7,1	4590	30	3490–3340	3500–3110
H6	8719	17	Male	Adult	Bone	Cranium	Beta-533971	41,7	15,2	3,2	–19,0	9,5	4510	30	3345–3105	3355–3100
H6	8132	2	Unknown	Adult	Bone	Cranium	Beta-571869	41,3	14,9	3,2	–19,10	9,0	4500	30	3340–3105	3350–3095
H6	8697	13	Unknown	Non-adult	Bone	Cranium	Beta-533967	42,3	15,4	3,2	–19,30	8,6	4500	30	3340–3105	3350–3095
H6	8251	9	Unknown	Adult	Bone	Cranium	Beta-533963	41,5	15,0	3,2	–18,40	10,8	4490	30	3330–3100	3350–3035
H6	8703	16	Female	Adult	Bone	Cranium	Beta-533970	41,1	14,7	3,3	–19,50	8,2	4480	30	3330–3100	3340–3030
H6	8698	14	Female	Adult	Bone	Cranium	Beta-533968	40,8	14,7	3,2	–19,90	8,8	4480	30	3330–3100	3340–3030
H6	8263	10	Male	Adult	Bone	Cranium	Beta-533964	41,1	14,9	3,2	–19,30	9,4	4470	30	3330–3040	3340–3025
H6	8701	15	Male	Adult	Bone	Cranium	Beta-533969	40,8	14,7	3,2	–19,30	9,7	4470	30	3330–3045	3340–3025
H6	8151	5	Unknown	Adult	Bone	Cranium	Beta-533960	41,7	15,0	3,2	–19,60	8,8	4470	30	3330–3045	3340–3025
H6	8758	8	Indeterminate	Adult	Bone	Cranium	Beta-533972	41,7	14,8	3.3	–19,60	7,6	4470	30	3330–3040	3340–3025
H6	8778	18	Female	Adult	Bone	Cranium	Beta-533973	41,5	14,9	3,2	–19,80	8,7	4470	30	3330–3040	3340–3025
H6	8671	12	Unknown	Non-adult	Bone	Cranium	Beta-533966	40,4	14,4	3,3	–19,90	7,8	4470	30	3330–3045	3340–3025
H6	8052-1	19	Unknown	Adult	Bone	Femur	Beta-571868	41,0	14,8	3,2	–20,10	6,5	4470	30	3330–3040	3340–3025
H6	8184	6	Indeterminate	Adult	Bone	Cranium	Beta-533961	41,6	14,9	3,2	–19,20	9,2	4460	30	3325–3030	3335–3020
H6	8185	7	Male	Adult	Bone	Cranium	Beta-533962	40,9	14,7	3,3	–18,90	9,0	4450	30	3320–3025	3335–2935
H6	8137	4	Unknown	Adult	Bone	Cranium	Beta-571871	39,8	14,3	3,2	–19,30	8,2	4450	30	3320–3025	3335–2935
H6	8035	20	Unknown	Adult	Bone	Cranium	Beta-501114	41,4	15,5	3,1	–19,90	8,0	4440	30	3315–3020	3330–2930
H6	8120	3	Unknown	Adult	Bone	Cranium	Beta-533959	41,2	14,8	3,2	–19,60	8,9	4380	30	3020–2925	3090–2910

This statistical study also identified outliers among each hypogeum as well as for the overall sample by applying OxCal's *Outlier Model* (Bronk Ramsey 2009b). The level of contemporaneity between the different ^{14}C measurements was tested by *Chi square tests* (Ward and Wilson 1978) which assessed the degree of overlapping among the ranges of probability. Non-parametric statistical methods based on *kernel density estimation* (KDE) (Bronk Ramsey 2017) were then applied as exploratory devices to characterise the potential phases of La Beleña's burials. This is a widely used frequentist method with no formal priors for the distribution. Its advantage when compared to that of the sum function is that it reduces the noise from the calibration procedure allowing KDE distribution to serve as a prior in the Bayesian model (Bronk Ramsey 2017). Furthermore, this method is more precise when lacking reliable information as to the stratigraphic relationship of the samples (Bronk Ramsey 2017). This is the case of La Beleña's hypogea marked by little reliable stratigraphic or spatial information due to the commingling and disarticulation of the human remains during multi-stage burial practices (Blank et al 2020). This was specifically carried out with KDE_Plot OxCal tools (Bronk Ramsey 2017).

Results

Isotopes analyses

Bone collagen samples was successfully extracted from 71 humans (52 bones and 19 teeth). The carbon and nitrogen content of both bone and dentine collagen ranged respectively from 20.7% to 45.48% (40.8% ± 3.2) and 7.4 to 16.46% (14.6% ± 1.2) (Table 2). The atomic C/N ratio ranged from 3.1 to 3.6 (3.2 mean) yielding acceptable atomic carbon/nitrogen ratios (van Klinken 1999; DeNiro 1985). The $\delta^{13}C$ values were between –20.49‰ and –18.4‰ (–19.5‰ ± 0.5, n = 71). Seven individuals yielded $\delta^{13}C$ values above –19‰. The $\delta^{15}N$ values, in turn, ranged between +6.98‰ and +11.62‰ (8.7‰ ± 1.1‰, n = 71). Three samples revealed $\delta^{15}N$ values >10‰ (Table 2). These results suggest that the diet was predominately terrestrial as $\delta^{13}C$ values were more negative than –18‰ and $\delta^{15}N$ values falling below 2‰ (Schulting et al 2024). Such isotopic signatures are consistent with those found in other Late Neolithic Iberian populations with terrestrial diets (Cubas et al 2019). It is noteworthy to mention that La Beleña is located at a distance of approximately 84 km from the Mediterranean Sea (Figure 1).

The general chronology of the Cemetery of La Beleña

Analyses of the overall sample (n = 71) yielded four early ^{14}C dates from Hypogeum 5: Beta-593540, Beta-593546, Beta-593548 and Beta-593547 (Table 2; Figure S1). However, when considering only the ^{14}C dates of Hypogeum 5, the results suggest that three ^{14}C dates pertain to an initial phase of burial activity, while the sample Beta-593540 appears to be an earlier outlier (Figure S2). Interestingly, the associated stable isotopic values for this individual do not indicate any reservoir effect on the ^{14}C date ($\delta^{13}C = –19.9‰$ and $\delta^{15}N = +9.4‰$).

The KDE model depicts a first phase of funerary activity around cal BC 3700 (Figure 3) followed by a short gap preceding another second phase of activity. The first phase comprises the three oldest ^{14}C dates of Hypogeum 5 (Beta-593546, Beta-593548 and Beta-593547) ranging from cal BC 3700–3450. The second cluster, after the short hiatus, comprises the group of datings from cal BC 3400 to 2900. The end of this second range most likely corresponds to the abandonment of the cemetery (Table 3). The KDE analyses therefore indicate a first phase linked to Hypogeum 5 and a second intensive burial phase between cal BC 3400 to 2900 comprising all the tombs. Thus, the Bayesian single model of the overall sample, when excluding the outlier, suggests that burials at Beleña began in *cal BC 3595–3540* (2σ; median = 3560) and ended in *cal BC 2915-2865* (2σ; median = 2895) separated by an interval of about 670 years (635–712 years, 2σ) (Table 3, Figure S3).

https://doi.org/10.1017/RDC.2024.64 Published online by Cambridge University Press

Table 3. *Multi-phase Bayesian ranges pertaining to the estimated start, span, interval and end of burials at La Beleña*

Model	Parameter	1σ	2σ	μ	σ	Median	A_{model}	$A_{overall}$
La Beleña	Start	3560–3560	3595–3540	3560	20	3560		
	Span	635–660	625–680	650	15	650		
	Interval	650–680	635–715	670	20	665	69.7	69.4
	End	2840–2825	2870–2800	2840	15	2840		
Beta-593540		4215–3990	4230–3980	4080	75	4050		
Phase 1 (n = 3)	Start	3730–3635	3975–3540	3710	140	3670		
	Span	0–110	0–145	50	45	35		
	Interval	0–175	0–515	150	180	105	97.3	88.1
	End	3640–3510	3645–3390	3533	75	3565		
Phase 2 (n = 67)	Start	3365–3285	3380–3175	3310	50	3315		
	Span	370–460	270–475	390	65	405		
	Interval	375–475	275–495	400	70	415		
	End	2910–2885	2995–2870	2905	25	2900		
Difference P1-P2		175–335	40–415	245	85	250		

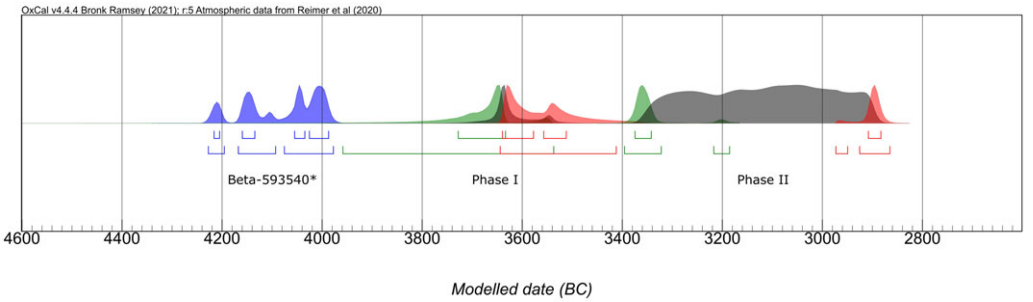

Figure 3. *La Beleña: KDE modeling of the ^{14}C datings. The graph depicts the two main burial phases and the outlier Beta-593540. The start boundaries are indicated in green, and the end boundaries in red. The outlier 14C date is highlighted in blue. Upper brackets below each age estimate represent the 68.2% and the lower brackets the 95.4% confidence interval.*

Bayesian analyses of the two funerary phases

A model illustrating the overlap of the two phases was drafted to further delve into the two main clusters of ^{14}C dates yielded by the KDE model (Figure 3). As the ^{14}C dates of Phase 1 pass the chi-square test (T' = 4.5 [T(5 % = 6.0)]) (Ward and Wilson 1978), it is possible to assume that the individuals likely died over a relatively short timespan (one or two generations) (Figure S4). Phase 1 thus begins around *cal BC 3975–3540* and ends between *cal BC 3645 and 3390* (2σ; median = 3710) within an interval of 0–515 (2σ; median = 150 years) (Table 3). The range between the end of Phase 1 and the outset of Phase 2 is estimated at between 40 and 415 years (2σ; median = 250 years) (Table 3). Phase 2 began around *cal BC 3380–3175* (2σ; median = 3305) and ended between *cal BC 2995–2870* (2σ; median = 2905) with an estimated interval of 185 and 500 years (2σ; median = 400 years) (Table 3).

https://doi.org/10.1017/RDC.2024.64 Published online by Cambridge University Press

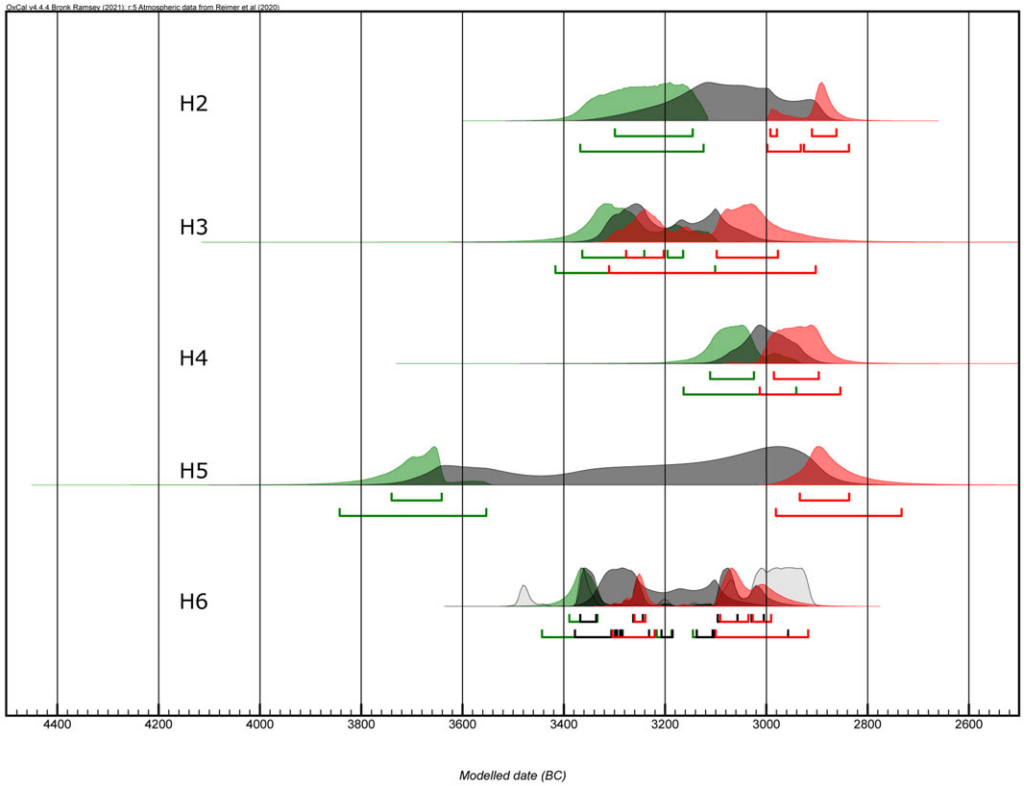

Figure 4. *Bayesian chronological ranges depicting the start and end of each hypogeum combined with individual KDE plots. The start boundaries are indicated in green, and the end boundaries in red. The outlier ^{14}C date is highlighted in blue. Upper brackets below each age estimate represent the 68.2% and the lower brackets the 95.4% confidence interval.*

Bayesian analyses of each hypogeum

Hypogeum 2

The ^{14}C dataset of Hypogeum 2 (n = 21) did not pass the chi-square test of contemporaneity (T' = 96.27 [T(5 % = 31.4)]) (Ward and Wilson 1978). This suggests that this ^{14}C dataset likely reflects multiple depositional events of human remains. Furthermore, no hiatus was discerned as in the KDE model (Figure 4; Figure S5). The Bayesian model indicates that the burial activity began in *cal BC 3370–3130* (2σ; median = 3250) and ended in *cal BC 3000–2835* (2σ; median = 2890) with an interval of 130–500 years (2σ; median = 360 years) (Table 4).

Hypogeum 3

The KDE model (n = 7) and the test of contemporaneity suggest that all the individuals in Hypogeum 3 were buried over a period of one or two generations (T' = 10.5 [T(5 % = 12.6)]) (Ward and Wilson 1978) (Figure 4; Figure S6). The burial practice began between *cal BC 3420–3100* (2σ; median = 3290) and ended between *cal BC 3310–2900* (2σ; median = 3070) with an interval of about 0–460 years (2σ, median = 150) (Table 4).

Hypogeum 4

The nine ^{14}C dates of Hypogeum 4 also did not pass the test of statistical contemporaneity (T' = 21.5 [T(5 % = 15.5)]) (Ward and Wilson 1978) (Figure 4; Figure S7). The model tends to offer younger dates

https://doi.org/10.1017/RDC.2024.64 Published online by Cambridge University Press

Table 4. *Single phase ranges for the estimated start, span, interval and end of each hypogeum*

Model	Parameter	1σ	2σ	μ	σ	Median	A_{model}	$A_{overall}$
H2	Start	3320–3170	3370–3130	3250	70	3250	86.8	80.7
	Span	260–420	130–450	320	80	330		
	Interval	280–460	130–500	350	100	360		
	End	2910–2860	3000–2835	2900	40	2890		
H3	Start	3370–3170	3420–3100	3280	90	3290		
	Span	0–170	0–300	130	90	110		
	Interval	0–250	0–460	180	150	150		
	End	3280–2980	3310–2900	3100	120	3070		
H4	Start	3110–3030	3160–2940	3070	55	3070		
	Span	40–150	0–190	100	55	100		
	Interval	40–190	0–270	130	80	120		
	End	2985–2900	3015–2855	2935	45	2940		
H5	Start	3740–3640	3840–3550	3700	70	3690		
	Span	695–780	630–805	725	45	730		
	Interval	730–900	650–1060	830	100	820		
	End	2940–2840	2980–2730	2870	65	2890		
H6	Start	3390–3330	3440–3100	3340	70	3360		
	Span	60–300	0–320	180	95	220		
	Interval	70–360	0–400	220	120	270		
	End	3260–2990	3310–2930	3100	105	3070		

for samples such as Beta-465699 and Beta-593538 which coincide with a plateau in the calibration curve. These factors may in fact affect the accuracy of the start of the depositions in this tomb. The model places the start of the burial activity sometime between *cal BC 3160–2940* (2σ; median = 2940) and the end around *cal BC 3015-2855* (2σ; median = 3065). The interval is estimated to between 0–270 years (2σ; median = 120 years) (Table 4).

Hypogeum 5

The results of the ^{14}C analyses of Hypogeum 5 did not pass the chi square test of contemporaneity (T' = 1105.1 [T(5 % = 23.7)]). This remained the case even when the outlier was excluded (T' = 520.3 [T(5 % = 22.5)]) (Ward and Wilson 1978). Moreover, the KDE model highlights the outlier and two distinct sets of datings (Figure 4). This led to the design of two Bayesian models, one of a single phase (Figure S8) and a second of two phases (Figure S9), excluding the outlier (Beta-593540). The first indicates an outset of burial activity between *cal BC 3840–3550* (2σ; median = 3690) and an end between *cal BC 2980–2730* (2σ; median = 2890) within an interval of 650–1060 years (2σ; median = 820 years) (Table 4).

The Bayesian model of the two phases of Hypogeum 5, excluding the outlier, reveals a first set of datings (Beta-593546, Beta-593547 and Beta-593548) corresponding to Phase 1 and the remaining to Phase 2. Those of Phase 1 pass the statistical test of contemporaneity (T' = 4.5 [T(5 % = 6.0)]) (Ward and Wilson, 1978). Those of Phase 2, on the contrary, do not (T' = 84.6 [T(5 % = 18.3)]) (Ward and Wilson 1978). The Bayesian model suggests that Phase 1 began between *cal BC 3980–3540* (2σ; median = 3670) and ended between *cal BC 3650–3260* (2σ; median = 3560) within an interval of 0–650 years (2σ, median = 110 years) (Table 5). Phase 2, in turn, began between *cal BC 3430–3120* (2σ; median = 3240) and ended between *cal BC 3000–2810* (2σ; median = 2910), with an interval of 150–590 years (2σ; median = 330 years). The difference between phases 1 and 2 was estimated at between 40–500 years (2σ; median = 305 years) (Table 5, Figure 5).

https://doi.org/10.1017/RDC.2024.64 Published online by Cambridge University Press

Table 5. *Results of the Bayesian multi-phase model of Hypogeum 5 indicating the ranges for its estimated start, span, interval and end*

Model	Parameters	1σ	2σ	μ	σ	Median	A_{model}	$A_{overall}$
Phase 1 (n = 3)	Start	3730–3630	3980–3540	3710	130	3670		
	Span	0–110	0–145	55	45	35		
	Interval	0–190	0–650	180	230	110		
	End	3640–3510	3650–3260	3530	130	3560		
Phase 2 (n = 11)	Start	3370–3140	3430–3120	3260	90	3240	108.3	95.7
	Span	180–450	150–460	290	90	280		
	Interval	200–430	150–590	350	120	330		
	End	2960–2870	3000–2810	2910	50	2910		
Difference P1-P2		170–410	50–470	270	110	280		

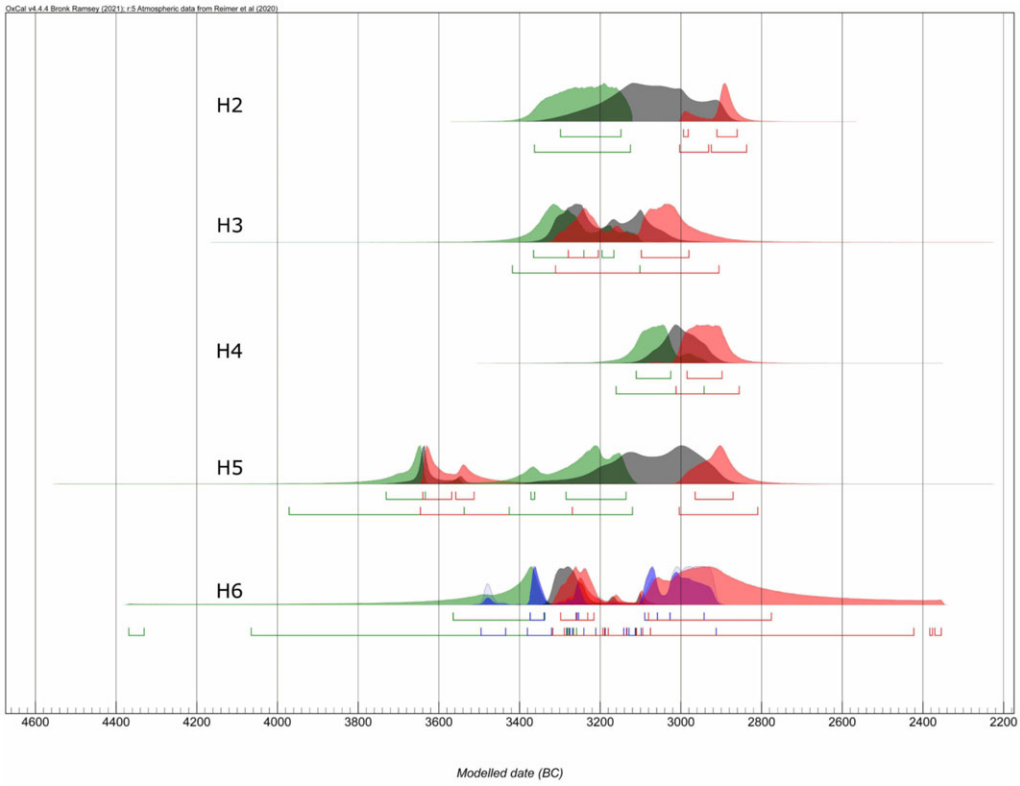

Figure 5. *Multi-phase Bayesian chronological ranges indicating the start and end of each phase and KDE plots of the overall distribution of dated events within each collective burial. Hypogeum 6 also includes high posterior densities of the oldest and youngest ^{14}C dates of the dataset (Table 6). The start boundaries are indicated in green, and the end boundaries in red. The outlier ^{14}C date is highlighted in blue. Upper brackets below each age estimate represent the 68.2% and the lower brackets the 95.4% confidence interval.*

https://doi.org/10.1017/RDC.2024.64 Published online by Cambridge University Press

Table 6. *Results of the Bayesian model for Hypogeum 6 indicating the ranges of the start, span, interval and end of its main phase of burial activity. The list includes the ranges of the oldest and youngest datings as well as the gaps between the main phase of burial activity, the end of the oldest (difference 1) and start of the youngest (difference 2)*

Model	Parameters	1σ	2σ	μ	σ	Median	A_{model}	$A_{overall}$
Beta-5333965		3485–3350	3500–3330	3400	60	3370		
Phase 1 (n = 17)	Start	3330–3275	3350–3170	3290	45	3300		
	Span	0–55	0–155	50	45	35		
	Interval	0–65	0–180	55	55	40	160.8	158.7
	End	3290–3220	3320–3085	3240	52	3250		
Beta-5333959		3020–2925	3090–2910	2990	50	2985		
Difference 1		20–195	5–230	110	70	85		
Difference 2		200–340	80–375	250	70	260		

Hypogeum 6

The assemblage of ^{14}C dates (n = 19) of Hypogeum 6 also did not pass the chi-square test of contemporaneity (T' = 31.1 [T(5 % = 28.9)]) (Ward and Wilson 1978). This may be due to the results of samples Beta-5333965 and Beta-5333959, yielding respectively the oldest and youngest dates. It is noteworthy that the KDE models depict a first peak based on sample Beta-5333965, a short gap, and then, the probabilistic distributions of the other ^{14}C results (Figs. 4–5). In any case, the Bayesian single model places the start of burial activity in this hypogeum between *cal BC 3440–3100* (2σ; median = 3360), the end between *cal BC 3310–2930* (2σ; median = 3070) and the interval between 0–400 years (2σ; median = 270 years) (Table 4; Figure S10).

The results indicate that 17 ^{14}C dates (89% of those of Hypogeum 6) yielded similar ranges and thus passing the chi-square test of contemporaneity (T' = 6.2 [T(5 % = 26.3)]) (Ward and Wilson 1978). They therefore suggest that the 17 individuals in its chamber died over a very short period of time. A Bayesian model was thus designed to delve into this cluster as a phase while maintaining Beta-533965 and Beta-533959 within the general model (Table 6; Figure 5). The results of Beta-533965 suggest the range of *cal BC 3500–3330* (2σ; median = 3370). Phase 1, in turn, began between *cal BC 3350–3170* (2σ; median = 3370) and ended sometime around *cal BC 3320–3085* (2σ; median = 3250) with an interval of 0–180 years (2σ; median = 40 years) (Table 6), whereas the modeled range of Beta-5333959 is *cal BC 3090–2910* (2σ; median = 2985) (Figure S11). Therefore, the model reinforces the notion that these 17 individuals met their death in a brief timeframe.

Discussion

The chronological sequence of the hypogea of La Beleña

Maximising the number of AMS ^{14}C dates (71 of 79 individuals, 90%) was a deliberate choice as they facilitate the understanding the prehistoric cemetery's different depositional events. Applying the fine-grained radiometric protocol enabled garnering notions as to patterns of burial activity with a precision corresponding to few human generations (Blank et al 2020; Scarre 2010; Wysocki et al 2013). Moreover, combining the data with the Bayesian modelings also increased the precision of the sequence offering a better understanding of the succession of the burial activity. Thus, the cemetery of La Beleña was inaugurated by hollowing out Hypogeum 5 and the deposit in it of the first human remains around cal BC 3700 (start of Phase 1). However, the findings include a ^{14}C date on a cranium from the same hypogeum that is distinctly earlier than the primary dataset of La Beleña. This date is identified as an outlier because it does not correspond with the remaining ^{14}C dates associated with the site's sequential deposition history. A viable hypothesis for this inconsistency is that the cranium might be a bone relic

https://doi.org/10.1017/RDC.2024.64 Published online by Cambridge University Press

utilised in the funerary practices of La Beleña. Bone relics are curated human remains that are subjected to intricate processes of dissemination, circulation, and re-disposal. Although the employment of bone relics in the funerary contexts of European Late Prehistory is relatively infrequent, it is not exceptional, becoming more common during the Bronze Age (Bradley 1998; Brück 2006; Esparza-Arroyo et al 2018; Fowler 2004). Such relics often play a crucial role in shaping identities and preserving social memory (Borić 2003; Lillios 1999; Weiss-Krejci 2011). Fundamentally, relics can be interpreted as tangible manifestations of memory, serving as a bridge between past and present, and between the realms of the living and the deceased (Walsham 2010). In the context of La Beleña, it is essential to note that this bone relic was found in the earliest hypogeum of the cemetery. Furthermore, the multi-stage burial practice at this site affords significant consideration to cranial remains, leading to the formation of skull caches within the burial space, as observed in hypogea 2, 4, and 6 (Figure 2; Camalich et al 2023). Therefore, it is possible that this cranium was involved in ritualistic practices intended to establish a connection between the deceased and their forebears by incorporating ancestral remains.

The initial surge of burial activity in La Beleña lasting around 40 years ended around cal BC 3550 (first phase of Hypogeum 5). Phase 2 saw the placing of new human remains around cal BC 3300 after a hiatus of ca. 250 years. It likewise coincided with another surge of burials in the form of the hollowing out of Hypogea 2, 3 and 6, and the reuse of Hypogeum 5. Individuals then continued to be deposited in Hypogea 2, 3 and 5, but not in Hypogeum 6. Ultimately, Hypogeum 4 was opened around cal BC 3065 cal while all the collective tombs, excepting Hypogeum 3, received new dead. The results therefore suggest a scaled construction of hypogea over time with new chambers were only inaugurated during more intense funerary activity. Both the archaeological evidence and the Bayesian models also reveal that all the tombs, except Hypogeum 3, were closed at about the same time (cal BC 2900, 2σ). The cemetery of La Beleña, undisturbed until its recent discovery in the 20th century, thus serves as a reliable indicator of the cycles of funerary activity linked to prehistoric collective tombs.

The statistical models indicate that Hypogea 2 and 5 saw use for hundreds of years by several generations. The funerary activity of Hypogeum 5 extended for about 730 years, a timespan significantly greater than that of Hypogeum 2 (ca. 330 years). On the contrary, the lifespans of Hypogeum 3 (ca. 145 years), Hypogeum 4 (ca. 100 years) and Hypogeum 6 (ca. 90 years) were relatively brief. The five collective tombs can, based on their duration, be classified into two groups: 1) Hypogea 2 and 5 followed by 2) Hypogea 3, 4 and 6. However, although group 1 saw a longer lifespan, the Bayesian analyses suggest that human remains arrived in the tombs during short, intense phases.

Hypogeum 5 saw two short-lived phases separated by a long hiatus (ca. 280 years). Phase 1 represents the initiation of funerary activity at La Beleña while Phase 2 is thought to correspond to a very intense period featuring the construction of Hypogea 2, 3 and 6. This surge is likewise observed at other Iberian prehistoric collective burials such as Alto Reinoso (Alt et al 2016), Cardim 6 (Valera et al 2019), Montelirio (García Sanjuán et al 2018), Los Zumacales (Santa Cruz del Barrio et al 2020), Panoría (Aranda Jiménez et al 2022) or Perdigoes 4 (Valera 2020b), among others. Other European megalithic assemblages such as the British monuments of Ascott-under-Wychwood (Bayliss et al 2007b) and Hazleton North (Meadows et al 2007), and the Swiss dolmen of Oberbipp (Ramstein et al 2022), also follow analogous patterns.

Up-to-date archaeological evidence suggests that this area saw limited settlement prior to the time frame associated with La Beleña (Martín Socas et al 2018). Yet, the significant funerary activity at this cemetery suggests emerging patterns of human occupation in the area during the latter half of the 4th millennium BC. While evidence for contemporary settlements in the immediate vicinity remains scarce, burial sites often serve as primary indicators of human activity (Camalich et al 2020; Martín Socas et al 2018). It is noteworthy that new sites contemporaneous with La Beleña have been discovered in the region, including Torreparedones (Martínez Sánchez et al 2014) and the Cave of Los Cuarenta (Vera Rodríguez et al 2014). Additional examples from more distant settings include the Polideportivo de Martos-La Alberquilla (Cámara et al 2010), Marroquíes Bajos (Portero et al 2010; Rodríguez Ariza 2011), and Loma de las Eras del Alcázar (Nocete et al 2009).

https://doi.org/10.1017/RDC.2024.64 Published online by Cambridge University Press

Other studies focusing on western and southwestern Iberia have likewise identified a rapid population growth between cal BC 3350 and 2900 based on Summed Probability Distributions (SPD) of ^{14}C dates (Balsera et al 2015; Lillios et al 2014; Pardo-Gordó and Carvalho 2020; Sweeney et al 2022). This growth coincides with the transition from the Late Neolithic to the Chalcolithic in southern Iberia, a process characterized by an intensification of food production (Cubas et al 2019), a development of permanent settlements (Díaz-del-Río 2023; Valera et al 2017) and an emergence of more complex social systems (Castro et al 1996; Díaz-del-Río 2023; García Sanjuán and Murillo-Barroso 2013; Gilman 1987a, 1987b). Palaeogenomic research also suggests biological exchanges between southern Iberia and northern Africa around cal BC 3000 (Fregel et al 2018). The dental non-metric trait analyses of southwestern Iberian populations of the Late Neolithic/Chalcolithic also reinforce the notion of arrivals from northwestern Africa and/or the eastern Mediterranean (Irish et al 2017). These biological findings are reinforced by discoveries of African ivory at Iberian Late Neolithic/Early Chalcolithic sites (Schuhmacher et al 2009). Therefore, the intensity of funerary activity at La Beleña coincides with a period in southern Iberia experiencing intense social transformations resulting in significant demographic growth.

The burst of funerary activity

The chi-square tests and the medians of the modeled distributions indicate that the earliest collective tomb of the cemetery, Hypogeum 5, experienced a brief rise in funerary activity (0–110, 1σ; 0–145, 2σ), followed by a hiatus of about 280 years. A similar pattern can be observed in Hypogeum 6 where 17 individuals likely died within a very short timespan between cal BC 3350–3170 and 3320–3090 (2σ), with an interval of 0–55 years (1σ) or 0–140 years (2σ). A similar short-lived increase of burials has been observed among other European collective tombs, such as Apeldoorn–Wieselse Weg and Garderen-Bergsham in the Netherlands (Bourgeois and Fontijn 2015), Knowth in Ireland (Schulting et al 2017), and West Kennet (Bayliss et al 2007c) and Wayland's Smithy I in England (Whittle et al 2007).

The sudden increase in burials within Hypogeum 6 may suggest that the corpses were deposited around the same time. However, due to the commingled and secondary nature of this burial, no stratigraphic relationship between them could be determined, leaving their synchronicity unresolved. Additionally, attempts to use ^{14}C dates to establish their synchronicity are limited by the precision of the technique, including issues with measurement errors, calibration curves, and statistical tools. This challenge also pertains to the ^{14}C dates of prehistoric mass graves in Spain (Alt et al 2020; Fernández-Crespo et al 2018), Germany (Meyer et al 2015) and Poland (Schroeder et al 2019) as their probability distributions did not reflect simultaneous interments due to the aforementioned issues. Indeed, the distributions of the 17 ^{14}C dates of La Beleña in fact reveal more restricted ranges than those of the mass graves. The systematic osteological analysis of the human remains did not yield any evidence of interpersonal or palaeopathological disorders in of La Beleña. Nevertheless, the absence of infectious disease-associated pathologies does not rule out the possibility of such diseases being responsible for the sudden and intense burial activity within Hypogeum 6. It is noteworthy that palaeogenomic evidence points to high-mortality epidemics among European Late Prehistory populations (Andrades Valtueña et al 2022; Rascovan et al 2019; Swali et al 2023). Indeed, the impact of *Yersinia pestis* can explain the decline of population during the Late Neolithic in northern Europe between cal BC 3000 and 2900 (Blank et al 2020; Feeser et al 2019; Sjögren et al 2019). Therefore, one cannot rule out that infectious diseases were behind the brief and intense burial activity of Hypogeum 6.

Conclusions

The modeled chronology suggests La Beleña to be one of the oldest rock-cut tomb or hypogeum cemeteries of the Iberian Peninsula. In fact, the first human depositions of Hypogeum 5 coincide with

https://doi.org/10.1017/RDC.2024.64 Published online by Cambridge University Press

the earliest Portuguese hypogea of Quinta da Abóboda, Barrancas I and Sobreira de Cima (Valera 2013, 2020a, 2020b). This type of funerary activity thus rapidly spread throughout southern Iberia. A similar rapid expansion of this tradition is observed in other regions of western Europe such as Provence where hypogea began to appear at around the same time (Sauzade 2021). The reasons and mechanisms behind this spread remain obscure. It does however coincide with more intense human mobility and long-distance exchanges observed from cal BC 3500 onwards (Díaz-del-Río 2023).

Burial activity at La Beleña then intensified around cal BC 3400–2900 (2σ). During this period, compelling evidence suggests a notable demographic growth stemming from agriculture intensification, population aggregation and the arrival of new groups from northwester Africa. The results of this study also suggest a brief surge of burials potentially related to catastrophic events such as an epidemic (Blank et al 2020). However, the limitations of the ^{14}C dating methods prevent delving deeper into this hypothesis. Furthermore, the modeled chronology of La Beleña reinforces the existence of multi-stage funerary practices (primary deposition, anthropogenic manipulations, secondary depositions, etc.) not only observed in these hypogea but among other types of collective tombs throughout western Europe such as barrows, cairns, and natural caves.

While further research is needed to refine the details of these notions, the sequence of the cemetery of La Beleña currently provides evidence of a rapid expansion of hypogea throughout southern Iberia. Yet the connections between the different areas of Western Europe characterised by these hypogea remain unclear. The influence of long-distance exchange and human migration on this funerary tradition is unexplored yet. However, these burial features and practices undoubtedly played a role in the social transformations that occurred during the transition from the Late Neolithic to the Chalcolithic. This study hence reinforces the idea that the tradition of multi-stage burials such as those observed among the hypogea of La Beleña also affected other types of European megalithic collective tombs.

Supplementary material. To view supplementary material for this article, please visit https://doi.org/10.1017/RDC.2024.64

Acknowledgments. This study was funded by the Ayuntamiento de Cabra (Córdoba) and Valora, Ltd. The fieldwork was authorised by the Andalusian government (Junta de Andalucía). This contribution was also supported by the research projects I+D "Producción y consumo. Las artesanías de las primeras sociedades campesinas en Andalucía Oriental entre el VI y el III milenio a.C. (MANOS)" (PID2019-104442GB-100) (MDC), RTI2018-101923-J-I00 (JS), RYC2019-028346 (JS), and CNS2022-136039 (JS) (Spanish Ministry of Science and Innovation). We also thank the editor and reviewers whose constructive comments greatly improved this manuscript.

References

Alt KW, Tejedor Rodríguez C, Nicklisch N, Roth D, Szécsényi Nagy A, Knipper C, Lindauer S, Held P, de Lagrán ÍGM, Schulz G, Schuerch T, Thieringer F, Brantner P, Brandt G, Israel N, Arcusa Magallón H, Meyer C, Mende BG, Enzmann F, Dresely V, Ramsthaler F, Guillén JIR, Scheurer E, López Montalvo E, Garrido Pena R, Pichler SL and Guerra MAR (2020) A massacre of early Neolithic farmers in the high Pyrenees at Els Trocs, Spain. *Scientific Reports* **10**, 2131.

Alt KW, Zesch S, Garrido-Pena R, Knipper C, Szécsényi-Nagy A, Roth C, Tejedor-Rodríguez C, Held P, García-Martínez-de-Lagrán Í, Navitainuck D, Arcusa Magallón H and Rojo-Guerra MA (2016) A community in life and death, the Late Neolithic Megalithic tomb at Alto de Reinoso (Burgos, Spain). *PLOS ONE* **11**, e0146176.

Andrades Valtueña A, Neumann GU, Spyrou MA, Musralina L, Aron F, Beisenov A, Belinskiy AB, Bos KI, Buzhilova A, Conrad M, Djansugurova LB, Dobeš M, Ernée M, Fernández-Eraso J, Frohlich B, Furmanek M, Hałuszko A, Hansen S, Harney É, Hiss AN, Hübner A, Key FM, Khussainova E, Kitov E, Kitova AO, Knipper C, Kühnert D, Lalueza-Fox C, Littleton J, Massy K, Mittnik A, Mujika-Alustiza JA, Olalde I, Papac L, Penske S, Peška J, Pinhasi R, Reich D, Reinhold S, Stahl R, Stäuble H, Tukhbatova RI, Vasilyev S, Veselovskaya E, Warinner C, Stockhammer PW, Haak W, Krause J and Herbig A (2022) Stone Age Yersinia pestis genomes shed light on the early evolution, diversity, and ecology of plague. *Proceedings of the National Academy of Sciences* **119**, e2116722119.

Aranda Jiménez G, Camalich Massieu MD, Martín Socas D, Díaz-Zorita Bonilla M, Hamilton D, Milesi L (2021) New insights into the radiocarbon chronology of Iberian megalithic societies, the Tholos-type tombs of Mojácar (Almería, Spain). *European Journal of Archaeology* **24**, 4–26.

Aranda Jiménez G, Díaz-Zorita Bonilla M, Hamilton D, Milesi García L and Sánchez Romero M (2020a) A radicocarbon dating approach to the deposition and removal of human bone remains in megalithic monuments. *Radiocarbon* **62**(5), 1147–1162.

Aranda Jiménez G, Díaz-Zorita Bonilla M, Hamilton D, Milesi García L, Sánchez Romero M (2020) The radiocarbon chronology and temporality of the megalithic cemetery of Los Millares (Almería, Spain). *Archaeological and Anthropological Science* **12**(5), 1–17.

Aranda Jiménez G, Lozano Medina Á, Camalich Massieu MD, Martín Socas D, Rodríguez Santos FJ, Trujillo Mederos A, Santana Cabrera J, Nonza-Micaelli A, Clop García X (2017) La cronología radiocarbónica de las primeras manifestaciones megalíticas en el sureste de la Península Ibérica, las necrópolis de Las Churuletas, La Atalaya y Llano del Jautón (Purchena, Almería). *Trabajos de Prehistoria* **74**, 257–277.

Aranda Jiménez G, Milesi García L, Hamilton D, Díaz-Zorita Bonilla M, Vílchez Suárez M, Robles Carrasco, S, Sánchez Romero, M, Benavides López, J.A (2022) The tempo of the Iberian megalithic rituals in the European context, The cemetery of Panoría. *Journal of Archaeological Science* **140**, 105579.

Balsera V, Díaz-del-Río P, Gilman A, Uriarte A and Vicent JM (2015) Approaching the demography of late prehistoric Iberia through summed calibrated date probability distributions (7000–2000 cal BC). *Quaternary International* **386**, 208–211.

Bayliss A (2009). Rolling out revolution, using radiocarbon dating in archaeology. *Radiocarbon* **51**, 123–147.

Bayliss A (2015) Quality in Bayesian chronological models in archaeology. *World Archaeology* **47**, 677–700.

Bayliss A, Benson D, Bronk Ramsey C, Galer D, McFayden L, van der Plicht J, Whittle A, Barclay A, Biddulph E, Case H, Clegg I, Copley M, Cramp K, Doherty C, Evans J, Evershed R, Grigson C, Guest P, Hedges R, Knüsel C, Limbrey S, Macphail R, Manning W, McFadyen L, Mulville J, Nimmo K, Pearson J, Roe F, Stevens R and Dennis I (2007b) Interpreting Chronology The Radiocarbon Dating Programme. In Benson D and Whittle (eds), *Building Memories*. Oxbow Books, 221–236.

Bayliss A, Bronk Ramsey C, van der Plicht J and Whittle A (2007a) Bradshaw and Bayes, towards a timetable for the Neolithic. *Cambridge Archaeological Journal* **17**, 1–28.

Bayliss A, Whittle A and Wysocki M (2007c). Talking about my generation, the date of the West Kennet Long Barrow. *Cambridge Archaeological Journal* **17**, 85–101.

Blank M, Sjögren K-G and Storå J (2020) Old bones or early graves? Megalithic burial sequences in southern Sweden based on ^{14}C datings. *Archaeological and Anthropological Sciences* **12**, 89.

Borić D (2003) "Deep time" metaphor, mnemonic and apotropaic practices at Lepenski Vir. *Journal of Social Archaeology* **3**, 46–74.

Boulestin B (2016) Qu'est-ce que le mégalithisme. In Jeunesse C, Le Roux P and Boulestin B (eds), *Mégalithismes Vivants et Passés, Approches Croisées; Living and Past Megalithisms, Interwoven Approaches*. Oxford: Archaeopress, 57–94.

Bourgeois QPJ and Fontijn DR (2015) The tempo of Bronze Age barrow use, modeling the ebb and flow in monumental funerary landscapes. *Radiocarbon* **57**, 47–64.

Bradley R (1998) Ruined buildings, ruined stones, enclosures, tombs and natural places in the Neolithic of south-west England. *World Archaeology* **30**, 13–22.

Bronk Ramsey C (2009a) Bayesian analysis of radiocarbon dates. *Radiocarbon* **51**, 337–360.

Bronk Ramsey C (2009b) Dealing with outliers and offsets in radiocarbon dating. *Radiocarbon* **51**, 1023–1045.

Bronk Ramsey C (2017) Methods for summarizing radiocarbon datasets. *Radiocarbon* **59**, 1809–1833.

Brück J (2006) Fragmentation, personhood and the social construction of technology in Middle and Late Bronze Age Britain. *Cambridge Archaeological Journal* **16**, 297–315.

Camalich Massieu MD, Rodríguez Santos FJ, Santana J, Caro Herrero JL, Martos Romero JA, Cacho Quesada C and Martín Socas D (2020) Implantación y desarrollo de las estrategias agropecuarias en el Sureste, la depresión de Vera (Almería). In Díaz del Río P, Lillios K and Sastre I (eds), *The Matter of Prehistory, Papers in Honor of Antonio Gilman Guillen. Bibliotheca Praehistorica Hispana XXXVI*. Madrid: Consejo Superior de Investigaciones Científicas, 173–192.

Camalich Massieu, MD, Santana J, Rodríguez Santos FJ, Goudiaby H, Caro Herrero JC, García González R, Cancel S, Caballero Crespo A and Martín Socas D (2023) La Necrópolis en hipogeo de La Beleña (Cabra, Córdoba), un hallazgo singular para comprender las prácticas funerarias del Neolítico Final en el suroeste europeo. In Rojo Guerra M and Díaz Navarro S (eds), *Las Tumbas y Los Muertos, Menga, Revista de Prehistoria de Andalucia, Monográfico 5*. Seville: Junta de Andalucía, 155–194.

Cámara Serrano JA, Riquelme Cantal JA, Pérez Bareas C, Lizcano Prestel R, Burgos Juárez A and Torres Torres F (2010) Sacrificio de animales y ritual en el Polideportivo de Martos–la Alberquilla (Martos, Jaén). *Cuadernos de Prehistoria y Arqueología de la Universidad de Granada* **20**, 295–327.

Carvalho AF (2014) *Bom Santo cave (Lisbon) and the middle Neolithic societies of southern Portugal*. Faro: Universidade do Algarve.

Castro P, Chapman R, Gili S, Lull V, Micó R, Rihuete C, Risch R and Sanahuja ME (1996) Teoría de las prácticas sociales. *Complutum Extra* **6**, 35–48.

Chambon P, Blin A, Bronk Ramsey C, Kromer B, Bayliss A, Beavan N, Healy F and Whittle A (2018) Collecting the dead, temporality and disposal in the Neolithic hypogée of Les Mournouards II (Marne, France). *Germania* **95**, 93–143.

Cook GT, Ascough PL, Bonsall C, Hamilton WD, Russell N, Sayle KL, Scott EM and Bownes JM (2015) Best practice methodology for ^{14}C calibration of marine and mixed terrestrial/marine samples. *Quaternary Geochronology* **27**, 164–171.

Cubas M, Peyroteo-Stjerna R, Fontanals-Coll M, Llorente-Rodríguez L, Lucquin A, Craig OE and Colonese AC (2019) Long-term dietary change in Atlantic and Mediterranean Iberia with the introduction of agriculture, a stable isotope perspective. *Archaeological and Anthropological Sciences* **11**, 3825–3836.

DeNiro MJ (1985) Postmortem preservation and alteration of in vivo bone collagen isotope ratios in relation to palaeodietary reconstruction. *Nature* **317**, 806–809.

Díaz-del-Río P (2023) Qué sucedió en la Edad del Cobre. *BSAA* LXXXVII, 164–243.

Esparza-Arroyo Á, Sánchez-Polo A and Velasco-Vázquez J (2018) Damaged burials or reliquiae cogotenses? On the accompanying human bones in burial pits belonging to the Iberian Bronze Age. *Archaeologies* **14**, 346–376.

https://doi.org/10.1017/RDC.2024.64 Published online by Cambridge University Press

Feeser I, Dörfler W, Kneisel J, Hinz M and Dreibrodt S (2019) Human impact and population dynamics in the Neolithic and Bronze Age, Multi-proxy evidence from north-western Central Europe. *The Holocene* **29**, 1596–1606.

Fernández-Crespo T, Schulting RJ, Ordoño J, Duering A, Etxeberria F, Herrasti L, Armendariz Á, Vegas JI and Bronk Ramsey C (2018) New radiocarbon dating and demographic insights into San Juan ante Portam Latinam, a possible Late Neolithic war grave in North-Central Iberia. *American Journal of Physical Anthropology* **166**, 760–771.

Fowler C (2004) *The Archaeology of Personhood, an Anthropological Approach*. London and New York: Routledge.

Fregel R, Méndez FL, Bokbot Y, Martín-Socas D, Camalich-Massieu MD, Santana J, Morales J, Ávila-Arcos MC, Underhill PA, Shapiro B, Wojcik G, Rasmussen M, Soares AER, Kapp J, Sockell A, Rodríguez-Santos FJ, Mikdad A, Trujillo-Mederos A, Bustamante CD (2018) Ancient genomes from North Africa evidence prehistoric migrations to the Maghreb from both the Levant and Europe. *Proceedings of the National Academy of Sciences* **1**, 6774–6779.

García Sanjuán L, Murillo-Barroso M (2013) Social complexity in Copper Age southern Iberia (ca. 3200–2200 cal BC), reviewing the "state" hypothesis at Valencina de la Concepción (Seville, Spain). In Berrocal MC, García Sanjuán L and Gilman A (eds), *The Prehistory of Iberia*. Routledge, 135–156.

García Sanjuán L, Vargas Jiménez JM, Cáceres Puro LM, Costa Caramé ME, Díaz-Guardamino Uribe M, Díaz-Zorita Bonilla M, Fernández Flores Á, Hurtado Pérez V, López Aldana PM, Méndez Izquierdo E, Pajuelo Pando A, Rodríguez Vidal J, Wheatley D, Bronk Ramsey C, Delgado-Huertas A, Dunbar E, Mora González A, Bayliss A, Beavan N, Hamilton D and Whittle A (2018) Assembling the dead, gathering the living, radiocarbon dating and Bayesian modelling for Copper Age Valencina de la Concepción (Seville, Spain). *Journal of World Prehistory* **31**, 179–313.

Gilman A (1987a) Regadío y conflicto en sociedades acéfalas. *BSAA* **LIII**, 59–72.

Gilman A (1987b) El análisis de clase en la Prehistoria del Sureste. *Trabajos de Prehistoria* **44**, 27–34.

Guilaine J (2015) *Les Hypogées Protohistoriques de la Méditerranée.* Arles: Arles et Fontvieille.

Guilaine J (2021) Mégalithes et grottes funéraires, Cohabitation? Complémentarité? Exclusion? Une histoire complexe. *Prehistoires Mediterranéennes* **9**, 11–20.

Gullì D and Terrasi F (2020) Nuove datazioni radiometriche da siti del territorio agrigentino e proposte per una sistematizzazione della cronologia dall'età del rame all'Età del Bronzo. *Vivere all'ombra del Vulcano*, 191.

Irish JD, Lillios KT, Waterman AJ and Silva AM (2017) "Other" possibilities? Assessing regional and extra–regional dental affinities of populations in the Portuguese Estremadura to explore the roots of Iberia's Late Neolithic–Copper Age. *Journal of Archaeological Science:Reports* **11**, 224–236.

Lillios KT (1999) Objects of memory, the ethnography and archaeology of heirlooms. *Journal of Archaeological Method and Theory* **6**, 235–262.

Lillios KT, Artz JA, Waterman AJ, Mack J, Thomas JT, Trindade L and Luna I (2014) The rock-cut tomb of Bolores (Torres Vedras), an interdisciplinary approach to understanding the social landscape of the Late Neolithic/Copper Age of the Iberian Peninsula. *Trabajos de Prehistoria* **71**, 282–304.

Linares-Catela JA and Vera-Rodríguez JC (2021) La cronología de la necrópolis de La Orden–Seminario (Huelva). Temporalidades de la actividad funeraria en las sepulturas del III milenio cal BC. *Trabajos de Prehistoria* **78**, 67–85.

Martín-Socas D, Camalich Massieu MD, Herrero JLC and Rodríguez-Santos FJ (2018) The beginning of the Neolithic in Andalusia. *Quaternary International* **470**, 451–471.

Martínez Sánchez RM, Pérez Jordá G, Peña-Chocarro L (2014) La campiña de Córdoba entre el IV y el I milenio ANE. Apuntes sobre la ocupación prehistórica del yacimiento de Torreparedones (Baena–Castro del Río, Córdoba). El sondeo 3, al norte del foro". *Antiqvitas* 26, 135–153.

Meadows J, Barclay A and Bayliss A (2007) A short passage of time, the dating of the Hazleton Long Cairn revisited. *Cambridge Archaeological Journal* **17**, 45–64.

Meyer C, Lohr C, Gronenborn D and Alt KW (2015) The massacre mass grave of Schöneck–Kilianstädten reveals new insights into collective violence in Early Neolithic Central Europe. *Proceedings of the National Academy of Science* **112**, 11217–11222.

Millard, A.R (2014) Conventions for Reporting Radiocarbon Determinations. *Radiocarbon* **56**, 555–559.

Nocete F, Lizcano R, Peramo A and Gómez E (2009) Emergence, collapse and continuity of the first political system in the Guadalquivir Basin from the fourth to the second millennium BC, The long–term sequence of Úbeda (Spain). *Journal of Anthropological Archaeology* **29**, 219–237.

Pardo-Gordó S and Carvalho AF (2020) Population dynamics during the Neolithic transition and the onset of megalithism in Portugal according to summed probability distribution of radiocarbon determinations. *Archaeological and Anthropological Sciences* **12**, 129.

Pestle WJ, Crowley BE and Weirauch MT (2014) Quantifying inter-laboratory variability in stable isotope analysis of ancient skeletal remains. *PLOS ONE* **9**, e102844.

Portero V, Serrano JL and Cano J (2010) Intervención arqueológica preventiva en la UE 17 de Jaén, centro comercial El Corte Inglés II. Anuario Arqueológico de Andalucía 2005, 2107–2118.

Ramstein M, Steuri N, Brönnimann D, Rentzel P, Cornelissen M, Schimmelpfennig D, Anselmetti FS, Häberle S, Vandorpe P, Siebke I, Furtwängler A, Szidat S, Hafner A, Krause J and Lösch S (2022) The well-preserved Late Neolithic dolmen burial of Oberbipp, Switzerland. Construction, use, and post-depositional processes. *Journal of Archaeological Science, Reports* **42**, 103397.

Rascovan, N, Sjögren, K-G, Kristiansen, K, Nielsen, R, Willerslev, E, Desnues, C, Rasmussen, S (2019) Emergence and Spread of Basal Lineages of Yersinia pestis during the Neolithic Decline. *Cell* 176, 295–305.e210.

https://doi.org/10.1017/RDC.2024.64 Published online by Cambridge University Press

Reimer PJ, Austin WEN, Bard E, Bayliss A, Blackwell PG, Ramsey CB, Butzin M, Cheng H, Edwards RL, Friedrich M, et al 2020. The IntCal20 Northern Hemisphere radiocarbon age calibration curve (0–55 cal kBP). *Radiocarbon* **62**(4), 725–757.

Robin G, Soula F, Tramoni P, Manca L and Lilley K (2021) "The dead are watching us", a landscape study of prehistoric rock-cut tomb cemeteries in Ossi, Sardinia, Italy. Proceedings of the Prehistoric Society 87, 1–30.

Rodríguez Ariza MO (2011) Evolución y uso de la vegetación durante la Prehistoria en el Alto Guadalquivir. *Menga, Revista de Prehistoria de Andalucía* **02**, 35–57.

Sánchez-Quinto F, Malmström H, Fraser M, Girdland-Flink L, Svensson EM, Simões LG, George R, Hollfelder N, Burenhult G, Noble G, Britton K, Talamo S, Curtis N, Brzobohata H, Sumberova R, Götherström A, Storå J and Jakobsson M (2019) Megalithic tombs in western and northern Neolithic Europe were linked to a kindred society. *Proceedings of the National Academy of Sciences* **116**, 9469–9474.

Santa Cruz del Barrio A, Villalobos García R and Delibes de Castro G (2020) Nueva serie de dataciones radiocarbónicas sobre hueso humano para el dolmen de Los Zumacales (Simancas, Valladolid). Reflexiones sobre la temporalidad del fenómeno megalítico en la Meseta Norte. *Trabajos de Prehistoria* **77**, 130–147.

Santana J (2020) Apuntes para el análisis e interpretación de contextos arqueológicos con restos óseos humanos. *Revista Atlántica–Mediterránea de Prehistoria y Arqueología Sociales* **21**, 29–55.

Sauzade G (2021) The collective burials of Provence in the long term. Permanence and evolution of the architectures and the funerary practices—abridged version. Préhistoires Méditerranéennes 9, 137–163.

Scarre C (2010) Rocks of ages, tempo and time in megalithic monuments. *European Journal of Archaeology* **13**, 175–193.

Scarre C, Laporte L and Joussaume R (2003) Long mounds and megalithic origins in western France, recent excavations at Prissé-la-Charrière. *Proceedings of the Prehistoric Society* **69**, 235–251.

Schroeder H, Margaryan A, Szmyt M, Theulot B, Włodarczak P, Rasmussen S, Gopalakrishnan S, Szczepanek A, Konopka T, Jensen TZT, Witkowska B, Wilk S, Przybyła MM, Pospieszny Ł, Sjögren K-G, Belka Z, Olsen J, Kristiansen K, Willerslev E, Frei KM, Sikora M, Johannsen NN and Allentoft ME (2019) Unraveling ancestry, kinship, and violence in a Late Neolithic mass grave. *Proceedings of the National Academy of Sciences* **116**, 10705–10710.

Schuhmacher TX, Cardoso João L and Banerjee A (2009) Sourcing African ivory in Chalcolithic Portugal. *Antiquity* **83**, 983–997.

Schulting RJ (2024) Dietary shifts at the mesolithic–neolithic transition in Europe: an overview of the stable isotope data. In Lee-Thorp J and Katzenberg MA (eds), *The Oxford Handbook of the Archaeology of Diet*, Oxford Handbooks, 297–332.

Schulting RJ, Bronk Ramsey C, Reimer PJ, Eogan G, Cleary K, Cooney G and Sheridan JA (2017) Dating the human remains from Knowth. In Eogan G and Cleary K (eds), *Excavations at Knowth 6, the Archaeology of the Large Passage Tomb at Knowth. Co. Meath*. Dublin: Royal Irish Academy, 331–385.

Schulz Paulsson B (2019) Radiocarbon dates and Bayesian modeling support maritime diffusion model for megaliths in Europe. *Proceedings of the National Academy of Sciences* **116**, 3460–3465.

Sjögren KG, Axelson T and Vretemark M (2019) Middle Neolithic economy in Falbygden, Sweden. Preliminary results from Karleby Logården. In *Megaliths, Societies, Landscapes, Early Monumentality and Social Differentiation in Neolithic Europe*. Proceedings of the international conference 16th–20th June 2015 in Kiel. Verlag Dr. Rudolf Habelt GmbH, 705–718.

Swali P, Schulting R, Gilardet A, Kelly M, Anastasiadou K, Glocke I, McCabe J, Williams M, Audsley T, Loe L, Fernández-Crespo T, Ordoño J, Walker D, Clare T, Cook G, Hodkinson I, Simpson M, Read S, Davy T, Silva M, Hajdinjak M, Bergström A, Booth T and Skoglund P (2023) Yersinia pestis genomes reveal plague in Britain 4000 years ago. *Nature Communications* **14**, 2930.

Sweeney L, Harrison SP and Linden MV (2022) Assessing anthropogenic influence on fire history during the Holocene in the Iberian Peninsula. *Quaternary Science Reviews* **287**, 107562.

Thompson JE, Parkinson EW, McLaughlin TR, Barratt RP, Power RK, Mercieca-Spiteri B, Stoddart S and Malone C (2020) Placing and remembering the dead in late Neolithic Malta, bioarchaeological and spatial analysis of the Xagħra Circle Hypogeum, Gozo. *World Archaeology* **52**, 71–89.

Valera AC (2013) A necrópole da Sobreira de Cima no contexto das práticas funerárias neolíticas no sul de Portugal, Sobreira de Cima. Necrópole de hipogeus do Neolítico (Vidigueira, Beja). *Lisbon, Era-Arqueologia SA (Era Monográfica)* 1, 113–129.

Valera AC (2020a) Absolute chronology of Vale de Barrancas 1 necropolis and the transition to collective burials in the Neolithic of South Portugal. In Valera AC and Nunes T (eds) Vale de Barrancas 1. A necrópole de hipogeus do Neolítico (Mombeja, Beja). Era Monográfica 4. Lisboa: Núcleo de Investigaçâo Arqueológica–NIA., 31–44.

Valera AC (2020b) O Sepulcro 4 dos Perdigões. Um tholos da segunda metade do 3° milénio AC, Perdigões Monográfica 2. Lisboa.

Valera AC, Figueiredo M, Lourenço M, Evangelista L, Basílio A and Wood R (2019) O Tholos de Cardim 6. Porto Torrão, Ferreira do Alentejo (Beja), Núcleo de Investigação Arqueológica (Nia) Era Arqueologia SA Lisboa.

Valera AC, Silva AM and Romero JEM (2014) The temporality of Perdigões enclosures: absolute chronology of the structures and social practices. *SPAL-Revista de Prehistoria y Arqueología* **23**, 11–26.

Valera AC, Simão I, Nunes T, do Pereiro T and Costa C (2017) Neolithic ditched enclosures in southern Portugal (4th millennium BC), new data and new perspectives. *Estudos do Quaternário/Quaternary Studies* **17**, 57–76.

van Klinken GJ (1999) Bone collagen quality indicators for palaeodietary and radiocarbon measurements. *Journal of Archaeological Science* **26**, 687–695.

Vera Rodríguez JC, Casas Flores MJ, Martínez Sánchez RM, Martínez Fernández MJ, Bretones García MD, Morgado Rodríguez A, López Flores I and Lozano Rodríguez JA (2014) Los contextos sepulcrales de la Cueva de los Cuarenta. Arqueología de los gestos funerarios durante la segunda mitad del IV milenio cal BC en el subbético cordobés. Antiqvitas 26, 71–133.

https://doi.org/10.1017/RDC.2024.64 Published online by Cambridge University Press

Walsham A (2010) Introduction: Relics and Remains, *Past & Present* **206**, 9–36.
Ward GK and Wilson SR (1978) Procedures for comparing and combining radiocarbon age determinations, a critique. *Archaeometry* **20**, 19–31.
Weiss-Krejci E (2011) The formation of mortuary deposits. In Agarwal SC and Glencross BA (eds), *Social Bioarchaeology*. Chichester: Wiley-Blackwell, 68–106.
Whittle A (2017) *Places of Special Virtue, Megaliths in the Neolithic Landscapes of Wales*, vol. **16**. Oxford: Oxbow Books, 1–224.
Whittle A, Bayliss A and Wysocki M (2007) Once in a lifetime, the date of the Wayland's Smithy Long Barrow. *Cambridge Archaeological Journal* **17**, 103–121.
Whittle A, Healy F and Bayliss A (2011) *Gathering Time, Dating the Early Neolithic Enclosures of Southern Britain and Ireland*. Oxford: Oxbow Books.
Wysocki M, Griffiths S, Hedges R, Bayliss A, Higham T, Fernandez-Jalvo Y and Whittle A (2013) Dates, diet, and dismemberment, evidence from the Coldrum Megalithic Monument, Kent. *Proceedings of the Prehistoric Society* **79**, 61–90.

Cite this article: Santana J, Caro JL, Camalich Massieu MD, Aranda Jiménez G, and Martín Socas D (2024). Sequencing the Southern Iberian Late Neolithic hypogeum cemetery of La Beleña through radiocarbon dating and Bayesian modeling. *Radiocarbon* **66**, 498–517. https://doi.org/10.1017/RDC.2024.64